

pubs.acs.org/JPCL Letter

# Preparation and Characterization of the Halogen-Bonding Motif in the Isolated Cl<sup>-</sup>·IOH Complex with Cryogenic Ion Vibrational Spectroscopy

Santino J. Stropoli, Thien Khuu, Joseph P. Messinger, Natalia V. Karimova, Mark A. Boyer, Itai Zakai, Sayoni Mitra, Anton L. Lachowicz, Nan Yang, Sean C. Edington, R. Benny Gerber,\* Anne B. McCoy,\* and Mark A. Johnson\*



Cite This: J. Phys. Chem. Lett. 2022, 13, 2750-2756



**ACCESS** 

Metrics & More

Article Recommendations

Supporting Information

**ABSTRACT:** In the presence of a halide ion, hypohalous acids can adopt two binding motifs upon formation of the ion—molecule complexes [XHOY] $^-$  (X, Y = Cl, Br, I): a hydrogen (HB) bond to the acid OH group and a halogen (XB) bond between the anion and the acid halogen. Here we isolate the X-bonded Cl $^-$ IOH ion—molecule complex by collisions of I $^-$ (H $_2$ O) $_n$  clusters with HOCl vapor and measure its vibrational spectrum by IR photodissociation of the H $_2$ -tagged complex. Anharmonic analysis of its vibrational band pattern reveals that formation of the XB complex results in dramatic lowering of the HOI bending fundamental frequency and elongation of the O $^-$ I bond (by 168 cm $^{-1}$  and 0.13 Å, respectively, relative to isolated HOI). The frequency of the O $^-$ I stretch (estimated 436 cm $^{-1}$ ) is also encoded in the spectrum by the weak  $\nu = 0 \rightarrow 2$  overtone transition at 872 cm $^{-1}$ .



 $\neg$  he isolated [XHOY] (X, Y = Cl, Br, I) ion-molecule complexes present the opportunity to investigate the competition between two well-known intermolecular interactions: hydrogen  $(HB)^{1-3}$  and halogen  $(XB)^{4,5}$  bonds. While the significance of HBs in chemical and biological systems cannot be overstated, the XB counterpart has attracted increasing attention due to its applications in drug design, crystal engineering, and catalysis.<sup>6-8</sup> The XB motif is commonly observed in condensed-phase systems,<sup>4</sup> and the molecular-level nature of the XB interactions between neutral molecules has been studied in detail through spectroscopic measurements on binary complexes such as H<sub>2</sub>O···ClF. The XB interaction is often characterized by using an electrostatic picture (Figure 1), in which the electron density surrounding a halogen atom that is covalently bound to an electronegative species (the XB donor) is anisotropically distributed. This creates an electropositive region (the "sigma hole") opposite its  $\sigma$  bond that can participate in an attractive interaction with a nucleophile (the XB acceptor). 4,5,10,11 Here we focus on the isolated anionic XB interaction involving a strong bond between a halide ion and a covalently bound halogen atom. An example of this motif is the recent capture of the Br-BrCCl<sub>3</sub> ion-molecule complex and its characterization using photoelectron spectroscopy. 12 Other schemes that have provided useful information about the XB interaction include molecular beam scattering, 13,14 ion-mobility measurements, 15,16 blackbody infrared radiative dissociation, 17 and

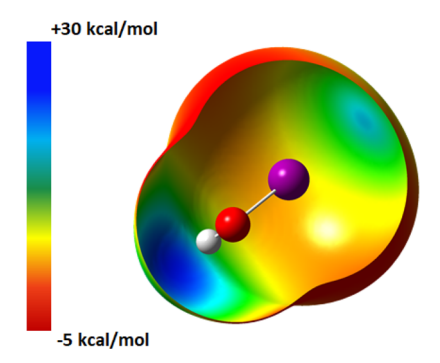


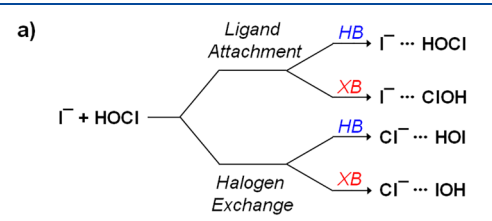
**Figure 1.** Electrostatic potential map of the HOI molecule calculated at the MP2/aug-cc-pVTZ level on a 0.001 e/bohr<sup>3</sup> surface. The electropositive "sigma hole" is shown in green, opposite the O–I bond. Units and sign conventions are based on those reported in ref 11.

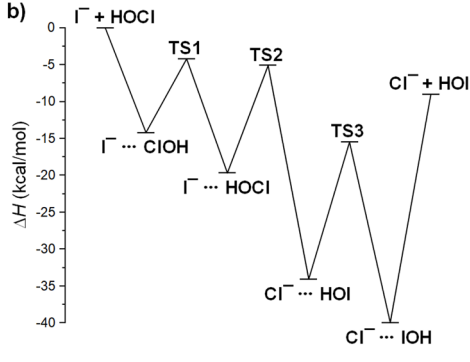
Received: January 22, 2022 Accepted: March 1, 2022



rotational spectroscopy. <sup>18–22</sup> In this report, we characterize the anionic XB interaction in the isolated Cl<sup>-</sup>·IOH ion—molecule complex using cryogenic ion vibrational spectroscopy.

Species with [IHOCl]<sup>-</sup> stoichiometry can occur in four distinct isomeric forms<sup>23</sup> shown schematically in Figure 2a.





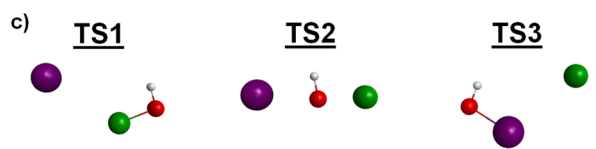


**Figure 2.** (a) Possible isomers of the [IHOCl]<sup>-</sup> ion-molecule complex. (b) Relative energy pathways (kcal/mol) for the rearrangement of each of the four possible [IHOCl]<sup>-</sup> isomers calculated at the MP2/aug-cc-pVTZ level of theory/basis, with transition states indicated as TS and transition state structures given in (c).

Two of these are the H- and X-bonded complexes based on the iodide, and the other two are based on chloride. All of these structures are calculated at the MP2/aug-cc-pVTZ level of theory/basis to be local minima in the potential energy surface with the Cl-IOH isomer lying lowest in energy as depicted in Figure 2b, followed by the two H-bonded forms, and then the I-ClOH species that adopts the least stable arrangement. Structures in which ICl is bound to OH were not found to be local minima. The H-bonded I-·HOCl isomer has recently been characterized with cryogenic vibrational spectroscopy (along with the Br-HOCl and Cl-HOCl analogues), <sup>24</sup> and its behavior conforms to established paradigms of strong anionic H-bonds.<sup>25</sup> Calculated partial charges (Table S1) demonstrate that the negative charge on I significantly increases from -0.48 e in I<sup>-</sup>·ClOH to -0.84 e in the more stable I<sup>-</sup>·HOCl (HB) form, which may also contribute to the larger binding energy of the latter. In this study, we isolate the X-bonded Cl<sup>-</sup>· IOH binary complex and characterize the XB interaction using cryogenic ion vibrational spectroscopy, electronic structure calculations performed at the MP2/aug-cc-pVTZ level (with the corresponding aug-cc-pVTZ-pp basis set and effective core <sup>27</sup> and anharmonic analysis of the vibrational potential for I),<sup>26</sup> level structure using an implementation of vibrational perturbation theory developed in one of our groups. 28,29

The [IHOCl]<sup>-</sup> binary complexes were prepared by reaction between gaseous HOCl and  $I^-\cdot(H_2O)_n$  cluster ions in the first quadrupole guide of the Yale cryogenic photofragmentation mass spectrometer as described in the Supporting Information. The dominant observed species correspond to the uptake of HOCl onto the parent  $I^-(H_2O)_n$  clusters to yield clusters with stoichiometry  $[IHOCl]^-\cdot(H_2O)_n$ . We focus here on the  $[IHOCl]^-$  product ion. One might expect that these products are primarily those arising from the so-called "ligand exchange" reaction:

$$X^{-}(H_2O)_n + HOCl \rightarrow X^{-}(HOCl) + nH_2O$$
 (1)

which was indeed the exclusive product channel when applied to the X = Cl and Br reactions. This was established by following the collisional breakup patterns:

$$X^{-}(HOCl) \rightarrow X^{-} + HOCl$$
 (2)

which only yield the halide ion from the reactant water clusters. In the case of X = I, however, breakup was observed to yield both halide ions:

$$[IHOCl]^{-} \rightarrow I^{-} + HOCl$$
 (3a)

$$[IHOCl]^{-} \rightarrow Cl^{-} + HOI \tag{3b}$$

with typical data included in Figure S2. As such, an additional mechanism is indeed occurring in the [IHOCl]<sup>-</sup> system. To explore why this pathway is available for the iodide case, we performed electronic structure calculations to evaluate the barriers for isomerization relative to that of the separated I<sup>-</sup> + HOCl reactants with the results indicated in Figure 2b. Inspection of the calculated stationary points on the potential surface describing the encounter of I<sup>-</sup> with HOCl indicates that reactive collisions between the bare species are sufficiently energetic to overcome the barriers in the overall exothermic ( $\Delta E = -9 \text{ kcal/mol}$ ) "halogen exchange" reaction:

$$I^- + HOCl \rightarrow Cl^- + HOI$$
 (4)

The calculated barriers for this reaction increase from  $X^- = I$  to Br to Cl (see Figure S3). Trapping the complexes in the various minima, on the other hand, requires collisional stabilization that is not available in the low-pressure environment of the ion guide. This can be accomplished, however, by evaporating one or more water molecules from the nascent collision complex:

$$I^{-}\cdot(H_{2}O)_{n} + HOCl \rightarrow [IHOCl^{*}]^{-}\cdot(H_{2}O)_{n}$$
  
 $\rightarrow [IHOCl]^{-} + nH_{2}O$  (5)

It is not clear at present whether the water molecule is chemically active in this process or simply serves as a third body to stabilize the collision complex. The fact that halogen exchange does not occur to an appreciable extent in the smaller halides is consistent with a scenario where they are initially formed in the H-bonded  $X^-\text{HOCl}$  well. From there, the increased barrier height to exchange as well as the increasing stability of the H-bonded  $X^-\text{HOCl}$  isomers acts to suppress conversion to other isomers. The  $X^-\text{HOCl}$  isomer energies relative to Cl $^-\text{XOH}$  isomers are calculated to be +20.3, + 3.3, and -9.9 kcal/mol for X = I, Br, and Cl, respectively (Figure S3). In a parallel study, the authors are currently pursuing *ab initio* molecular dynamics simulations of the halogen exchange reaction in bulk liquid water, the results of which show a mechanism that indeed depends on the participation of water

molecules. While the reaction dynamics of the cluster chemistry described here are indeed interesting, they fall outside the scope of the present report on the nature of the [IHOCl]<sup>-</sup> species generated in this process.

With both halide ions in play, it remains to be established which of the four possible isomers shown in Figure 2a are generated in the water cluster-mediated preparation. This was first addressed by acquiring the vibrational spectra of the cryogenically cooled ions in the OH stretching region. To accomplish this, the [IHOCl] products were transferred to a cryogenically cooled ( $\sim$ 20 K), 3D Paul Trap to enable condensation of hydrogen (H<sub>2</sub>) "tagging" molecules, and vibrational spectra were collected by monitoring the photoevaporation of these weakly bound adducts in a linear action mode:

$$[IHOCl]^-H_2 + h\nu \rightarrow [IHOCl]^- + H_2 \tag{6}$$

as has been previously described. 30-32

The vibrational spectrum of the H<sub>2</sub>-tagged [IHOCl]<sup>-</sup> ion is presented in Figure 3a. The feature highest in energy  $(v_{\rm H_2})$  is the H<sub>2</sub> fundamental, which gains intensity in the electric field of an ion.<sup>33</sup> The strongest feature, and the suite of vibrations that occur along with it, have been assigned to the H-bonded isomer with composition I-HOCl and were analyzed in a previous report.<sup>24</sup> The sharp band (denoted  $v_{OH_f}$  and highlighted in red) at 3641 cm<sup>-1</sup> was observed to be extremely weak in the ions created for that study but is much more intense in the species created for this work, consistent with its assignment to a second isomer. This is indeed the case, as confirmed by the isomer-selective, two-color IR-IR spectra displayed in Figures 3b and 3c. In that approach, 30,34 all features arising from a common carrier are identified by scanning a photobleaching laser while a second "probe" laser is tuned to a transition arising from one of the isomers present. All transitions in the spectrum associated with the isomer that is probed by the fixed laser appear as depletions or "dips" in the probe laser fragment signal as the bleaching laser is scanned across the entire spectral range. The two probe bands used here are indicated by the blue and red arrows in Figure 3a. Only two distinct band patterns were recovered, one of which corresponds to those arising from the I-HOCl, HB isomer reported earlier. The species responsible for the free OH band yields only this transition (besides  $v_{\rm H_2}$ ) in the entire region as shown in the photodepletion spectrum (Figure 3c). The single free OH band at 3641 cm<sup>-1</sup> falls close to the OH stretches in bare HOCl and HOI (black arrows at 360935  $(v_{\rm OH_f}^{\rm HOCl})$  and  $3620^{36}$   $(v_{\rm OH_f}^{\rm HOI})$  cm<sup>-1</sup>, respectively, in Figure 3a). The single free OH feature therefore signals the formation of an XB isomer, but it remains to be determined whether this species is based on I-, Cl-, or contributions from both ions based on the location of the observed band.

In a cursory survey experiment, we note that the propensity to generate the XB isomer increased with the center-of-mass collision energy between  $I^-\cdot(H_2O)_n$  and HOCl, supporting the notion that large initial internal energy is enabling interconversion followed by kinetic trapping by the cold buffer gas in the Paul trap. These speculations can be tested experimentally by systematically changing the  $I^-\cdot(\text{solvent})$  reactant to vary the strength of the H-bond and therefore tune the internal energies of the [IHOCl] $^-$  nascent product. Spectra that illustrate this kinetic control of the two isomers are displayed in Figure S4. However, the purpose of this study is to

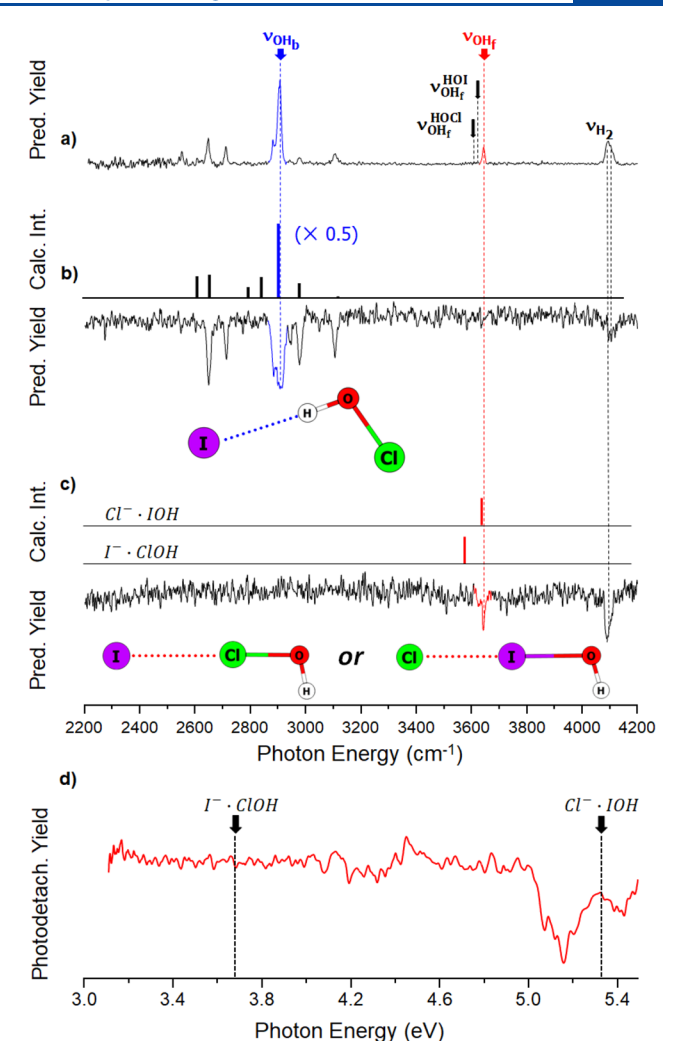


Figure 3. (b-c) Isomer-selective, two-color, IR-IR photobleaching spectra of the H<sub>2</sub>-tagged [IHOCl] vibrational predissociation spectrum. Two patterns are observed to contribute to the nonselective spectrum (a) by fixing the probe laser on the bands indicated by downward arrows at 2903 cm<sup>-1</sup> (blue) and 3641 cm<sup>-1</sup> (red) in (a). The pattern in (b) contains the strongly red-shifted OH fundamental and corresponds to the HB isomer (I-HOCl). The second pattern (c) consists of only a single feature at 3641 cm<sup>-1</sup>, which is the expected behavior of either the X-bonded Cl-IOH or I-ClOH isomers. Stick spectra calculated at the MP2/aug-cc-pVTZ level of theory/basis with anharmonic corrections<sup>28</sup> based on VPT2 calculations are presented above each experimental spectrum in (b) and (c) with minimum-energy structures inset. The literature values of the free OH stretching mode for neutral HOCl (ref 35,  $v_{OH_c}^{HOCl}$ ) and HOI (ref 36,  $v_{OH_c}^{HOI}$ ) are indicated by the black arrows in (a). Detailed assignments of the additional I-HOCl features and descriptions of the calculated stick spectra in (b) can be found in ref 24. (d) IR-UV photodetachment "dip" spectrum of the XB isomer obtained by IR photobleaching at 3641 cm<sup>-1</sup> as described in Section S1, where the black arrows indicate the estimated (see Table S5) electron affinity values for the two possible XB forms.

report that this interesting XB species can indeed be trapped and spectroscopically characterized by using the ligand exchange approach.

Unfortunately, it is not straightforward to distinguish between the two possible XB structures, namely Cl<sup>-</sup>·IOH or I<sup>-</sup>·ClOH, by the qualitative band pattern in the fingerprint region (vide infra) because their calculated spectra are similar

(see Tables S2 and S3), as was the case in the OH stretching region. It is therefore useful to seek an alternative method to establish the charge carrier. One property that is very different for the two complexes is the electron affinity (EA) of each complex, since the EA values of Cl and I differ by more than  $0.5 \text{ eV} (3.62^{37} \text{ vs } 3.06^{38} \text{ for Cl and I, respectively})$ . Because the binding energies of the neutral analogues are much smaller than those of the ions, the EAs of the complexes are shifted higher mostly by the binding energies,  $D_0$ , of the ions to the neutrals. The  $D_0$  values are calculated to be 1.73 and 0.62 eV for Cl-·IOH and I-·ClOH, respectively (see Figure S3). Correcting for the calculated neutral binding energies yields estimated EAs to be 5.35 and 3.68 eV for the Cl<sup>-</sup> and I<sup>-</sup> XB complexes, respectively (see Table S5). The electron affinities of the analogous halide complexes with water are wellknown,<sup>39</sup> and their photodetachment spectra display relatively sharp onsets<sup>40</sup> at the adiabatic EA according to the Wigner threshold laws for mostly s-wave detachment.

The measured photodetachment spectra of the [IHOCl] ions generated by different source conditions to enhance one isomer over the other are displayed in Figure S5. The photodetachment spectrum for the I-HOCl, HB isomer displays a less well-defined onset near 4 eV with some vibrational structure leading to a vertical detachment value of ~4.25 eV, which is consistent with the calculated threshold for this species at 3.91 eV. The threshold for the XB species is measured to be much higher, with an onset near 5 eV with a vertical value of  $\sim$ 5.1 eV, close to the calculated value for the Cl<sup>-</sup>, XB isomer of 5.35 eV. As a further proof of this conclusion, we also performed an IR photobleaching experiment to remove the XB isomer by excitation of the free OH band. The resulting difference photodetachment spectrum is displayed in Figure 3d and is indeed similar to that extracted by varying the relative populations of the isomers and monitoring changes in the overall photodetachment spectrum (Figure S6d). The calculated EAs of the possible isomers are indicated by arrows in Figure 3d, thus establishing that the species with the telltale free OH feature is based on the Clcharge carrier. We therefore conclude that the XB species generated in our ion source is in fact exclusively the Cl-IOH complex. We note that it is curious that we could not observe the Cl<sup>-</sup>·HOI, HB form of the [IHOCl]<sup>-</sup> complex, even though this is calculated to be separated by a substantial barrier from the Cl<sup>-</sup>·IOH, XB isomer. It is possible that a small yield of this HB complex is formed, but its strongly red-shifted OH stretch (to ~2300 cm<sup>-1</sup>, see Table S4) falls outside the range scanned here. Based on the spectral behavior of the  $X^-\cdot HOCl$ , (X = Cl, Br, I) series, however, we would expect to observe the HOI bending fundamental at ~1300 cm<sup>-1</sup> but do not. It is also noteworthy that we are unable to generate XB forms of either the [BrHOCl] or [ClHOCl] systems using the same experimental protocols that efficiently generate the Cl-IOH, XB species. As noted above, the Br $^{-}$ ·(H<sub>2</sub>O)<sub>n</sub> + HOCl reaction did not display halide exchange either. One possible explanation for this behavior is that in the case of reaction with  $I^-(H_2O)_n$ , the water molecules participate in the halide exchange mechanism through proton transfer. This is supported by molecular dynamics calculations which indicate that I reacts spontaneously to form Cl-IOH and that this species persists in the XB arrangement, while the Cl-HOI (HB) form does not, instead adopting a solvent-separated local arrangement rather than a direct HB to the acid HO group. This raises the interesting question regarding the chemical

nature of the  $[IHOCl]^-$  species that are present in the products of reaction 5 that retain water molecules ( $[IHOCl]^-$ ·  $(H_2O)_n$ ). These are prepared in abundance, and spectroscopic investigation of their composition is a promising direction for further work on this class of systems.

Having identified the Cl<sup>-</sup>·IOH halogen-bonded isomer, we next turn to the measurement of its vibrational spectrum arising from the lower frequency modes displayed in Figure 4.

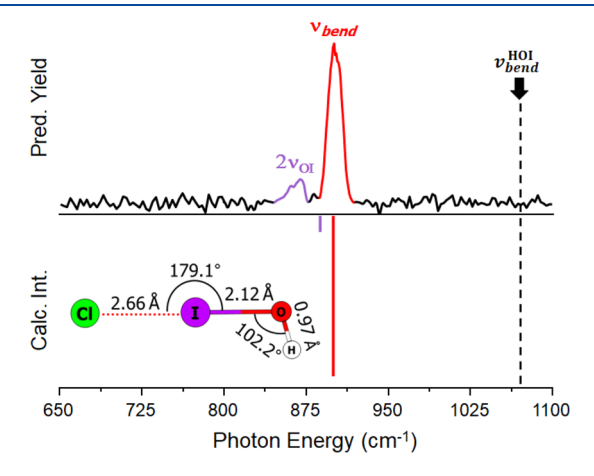


**Figure 4.** Low-frequency region of the experimental  $H_2$ -tagged  $Cl^-$ IOH vibrational predissociation spectrum, with the minimum-energy structure and corresponding inverted stick spectra calculated at the MP2/aug-cc-pVTZ level of theory/basis with anharmonic corrections based on VPT2 calculations presented below. The literature value <sup>36</sup> of the HOI bending mode for neutral HOI ( $\nu_{\rm bend}^{\rm HOI}$ ) is indicated by the black arrow.

The only bands observed in this frequency range of the Yale instrument (>600 cm<sup>-1</sup>) are an asymmetric doublet at around 900 cm<sup>-1</sup>. The dominant band at 902 cm<sup>-1</sup> is very close to the calculated value of the HOI bending mode in the Cl<sup>-</sup>·IOH complex (897 cm<sup>-1</sup>) and is therefore assigned to this fundamental. Note that this value lies far below the bend in the isolated HOI species<sup>36</sup> (1070 cm<sup>-1</sup>), immediately signaling an important aspect of the XB interaction in that the concomitant weakening of the OI bond acts to soften the potential for displacement of the OH bond angle. This is in sharp contrast to the HB interactions, which lead to an increase in the HOCl bend frequency by more than 100 cm<sup>-1</sup>.<sup>24</sup> The calculated and measured bend frequencies of various halogen- and hydrogen-bonded complexes of are provided in the Table S6.

The accurate recovery of the observed bending mode is important because it establishes a benchmark for the level of theory needed to treat this interaction. We note that this was accomplished using anharmonic methods that also yield predictions for nominally forbidden transitions such as overtones and combination bands. Indeed, the weaker feature at 872 cm<sup>-1</sup> appearing just below the bend fundamental is predicted (inverted purple bar in Figure 4) with about this relative intensity to be due to the  $\nu = 0 \rightarrow 2$  overtone of the low-frequency O–I stretching mode, which in turn indicates an approximate value for the fundamental of 436 cm<sup>-1</sup>.

Table 1 lists the experimental and calculated parameters for neutral HOX and the [IHOCl]<sup>-</sup> binary complexes. In the Cl<sup>-</sup>· IOH structure, the halide—halide Cl<sup>-</sup>···I bond lies along the O—I bond axis (Cl<sup>-</sup>···IO bond angle of 179.1°) and the interatomic Cl···I distance (2.67 Å) is dramatically shorter than

Table 1. Experimental (exp., Accurate to within  $\pm 4$  cm<sup>-1</sup>) and Calculated (calc., MP2/aug-cc-pVTZ with Anharmonic Corrections)<sup>28</sup> Frequencies (in Bold) and Calculated Structural Parameters for Neutral HOX (X = Cl, I) and the [IHOCl]<sup>-</sup> Complexes Reported in This Study, Where R is the Bond Length (Å) and  $\angle$  is the Bond Angle (deg)

parameter	HOCl	I⁻⋅HOCl	HOI	Cl⁻-IOH
exp. $v_{\mathrm{OH_b}}/v_{\mathrm{OH_f}}$ (cm <sup>-1</sup> )	3609 <sup>35</sup>	2903 <sup>24</sup>	3620 <sup>36</sup>	3641
calc. $v_{\mathrm{OH_b}}/v_{\mathrm{OH_f}}$ (cm <sup>-1</sup> )	3594	2903 <sup>24</sup>	3597	3636
exp. $v_{\rm bend}~({\rm cm}^{-1})$	1240 <sup>43</sup>	1341 <sup>24</sup>	$1070^{36}$	902
calc. $v_{\rm bend}$ (cm <sup>-1</sup> )	1228	1346 <sup>24</sup>	1069	897
$R_{\rm I \dots H}^- / R_{\rm Cl \dots I}^- (Å)$		2.30		2.67
$R_{\rm OCl} / R_{\rm OI}  (\rm \AA)$	1.70	1.69	1.99	2.12
$R_{\mathrm{OH}}$ (Å)	0.97	1.01	0.97	0.97
∠HOCl/∠HOI (deg)	102.5	103.2	104.2	102.3
$\angle I^- \cdots HO / \angle CI^- \cdots IO \text{ (deg)}$		176.3		179.1

the sum of the respective van der Waals radii (3.73 Å), both of which are key features in the recent IUPAC definition of a halogen bond. Additionally, the O–I bond distance (2.12 Å) is significantly lengthened relative to neutral HOI (1.99 Å), and there is a substantial calculated contraction of the internal HOI angle (102.3° vs 104.2° for neutral HOI). Interestingly, the free OH fundamental in the XB structure is blue-shifted (by 21 cm $^{-1}$ ) relative to HOI, suggesting enhancement of the electron density in the OH bond.

We have reported the capture of the halogen-bonded Cl-. IOH ion-molecule complex by halide exchange in the reaction between  $I^-(H_2O)_n$  clusters and HOCl vapor at low pressure in an quadrupole ion guide. Charge localization on the chloride was confirmed by monitoring the electron photodetachment threshold, while the XB docking arrangement was established by the observation of a free OH stretching transition close to that of the isolated HOI molecule. The low-frequency region of the spectrum features a strong band at 902 cm<sup>-1</sup> assigned to the HOI bending fundamental, which falls 168 cm<sup>-1</sup> below that of the bare HOI molecule. Anharmonic calculations enable assignment of the overtone of the O-I stretching mode, which provides an estimate of the fundamental value to be 436 cm<sup>-1</sup>. Calculated structures consistent with the observed bands yield a complete characterization of the isolated XB complex in addition to the overall potential energy landscape describing the relative energies and transition states separating the four isomers with stoichiometry [IHOCl]<sup>-</sup>.

## ASSOCIATED CONTENT

#### Supporting Information

The Supporting Information is available free of charge at https://pubs.acs.org/doi/10.1021/acs.jpclett.2c00218.

Detailed experimental and computational data (PDF)

#### AUTHOR INFORMATION

### **Corresponding Authors**

R. Benny Gerber — Department of Chemistry, University of California, Irvine, Irvine, California 92697, United States; Institute of Chemistry and the Fritz-Haber Center for Molecular Dynamics, The Hebrew University, Jerusalem 91905, Israel; orcid.org/0000-0001-8468-0258; Email: bgerber@uci.edu

Anne B. McCoy – Department of Chemistry, University of Washington, Seattle, Washington 98195, United States;

o orcid.org/0000-0001-6851-6634; Email: abmccoy@ uw.edu

Mark A. Johnson — Sterling Chemistry Laboratory, Department of Chemistry, Yale University, New Haven, Connecticut 06520, United States; oorcid.org/0000-0002-1492-6993; Email: mark.johnson@yale.edu

#### **Authors**

Santino J. Stropoli – Sterling Chemistry Laboratory, Department of Chemistry, Yale University, New Haven, Connecticut 06520, United States; orcid.org/0000-0003-4203-5060

Thien Khuu — Sterling Chemistry Laboratory, Department of Chemistry, Yale University, New Haven, Connecticut 06520, United States; orcid.org/0000-0003-0386-2450

Joseph P. Messinger – Sterling Chemistry Laboratory, Department of Chemistry, Yale University, New Haven, Connecticut 06520, United States; orcid.org/0000-0001-7305-3945

Natalia V. Karimova — Department of Chemistry, University of California, Irvine, Irvine, California 92697, United States; orcid.org/0000-0002-4616-1884

Mark A. Boyer — Department of Chemistry, University of Washington, Seattle, Washington 98195, United States Itai Zakai — Institute of Chemistry and the Fritz-Haber Center for Molecular Dynamics, The Hebrew University, Jerusalem

91905, Israel; orcid.org/0000-0002-0543-6562
Sayoni Mitra — Sterling Chemistry Laboratory, Department of Chemistry, Yale University, New Haven, Connecticut 06520, United States; orcid.org/0000-0003-4526-730X

Anton L. Lachowicz – Sterling Chemistry Laboratory, Department of Chemistry, Yale University, New Haven, Connecticut 06520, United States

Nan Yang — Sterling Chemistry Laboratory, Department of Chemistry, Yale University, New Haven, Connecticut 06520, United States; Occid.org/0000-0003-1253-2154

Sean C. Edington – Sterling Chemistry Laboratory,
Department of Chemistry, Yale University, New Haven,
Connecticut 06520, United States; orcid.org/0000-00025894-8801

Complete contact information is available at: https://pubs.acs.org/10.1021/acs.jpclett.2c00218

#### Notes

The authors declare no competing financial interest. Data used to generate figures is publicly available in a dataset hosted by the UCSD Library Digital Collections at: https://doi.org/10.6075/J03J3D4S.

## ACKNOWLEDGMENTS

This work was supported by NSF through the NSF Center for Aerosol Impacts on Chemistry of the Environment (CAICE), CHE-1801971. Any opinions, findings, and conclusions or recommendations expressed in this material are those of the author(s) and do not necessarily reflect the views of the National Science Foundation (NSF). Additionally, this work used the Extreme Science and Engineering Discovery Environment (XSEDE),<sup>44</sup> which is supported by Grant TG-CHE170064. A.B.M. acknowledges support from the Chemistry Division of the National Science Foundation (CHE-1856125 for scientific work and OAC-1663636 for perturbation theory code development). Parts of this work were performed by using the Ilahie cluster at the University of

Washington, which was purchased by using funds from a MRI grant from the National Science Foundation (CHE-1624430). This work was also facilitated through the use of advanced computational, storage, and networking infrastructure provided by the Hyak supercomputer system and funded by the STF at the University of Washington.

### REFERENCES

- (1) Jeffrey, G. A.; Saenger, W. Hydrogen Bonding in Biological Structures; Springer-Verlag: Berlin, 1991.
- (2) Scheiner, S. Hydrogen Bonding: A Theoretical Perspective; Oxford University Press: New York, 1997.
- (3) Arunan, E.; Desiraju, G. R.; Klein, R. A.; Sadlej, J.; Scheiner, S.; Alkorta, I.; Clary, D. C.; Crabtree, R. H.; Dannenberg, J. J.; Hobza, P.; Kjaergaard, H. G.; Legon, A. C.; Mennucci, B.; Nesbitt, D. J. Definition of the Hydrogen Bond (IUPAC Recommendations 2011). *Pure Appl. Chem.* **2011**, 83 (8), 1637–1641.
- (4) Cavallo, G.; Metrangolo, P.; Milani, R.; Pilati, T.; Priimagi, A.; Resnati, G.; Terraneo, G. The Halogen Bond. *Chem. Rev.* **2016**, *116* (4), 2478–2601.
- (5) Desiraju, G. R.; Ho, P. S.; Kloo, L.; Legon, A. C.; Marquardt, R.; Metrangolo, P.; Politzer, P.; Resnati, G.; Rissanen, K. Definition of the Halogen Bond (IUPAC Recommendations 2013). *Pure Appl. Chem.* **2013**, *85* (8), 1711–1713.
- (6) Scholfield, M. R.; Vander Zanden, C. M.; Carter, M.; Ho, P. S. Halogen Bonding (X-Bonding): A Biological Perspective. *Protein Sci.* **2013**, 22 (2), 139–152.
- (7) Gilday, L. C.; Robinson, S. W.; Barendt, T. A.; Langton, M. J.; Mullaney, B. R.; Beer, P. D. Halogen Bonding in Supramolecular Chemistry. *Chem. Rev.* **2015**, *115* (15), 7118–7195.
- (8) Li, B.; Zang, S. Q.; Wang, L. Y.; Mak, T. C. W. Halogen Bonding: A Powerful, Emerging Tool for Constructing High-Dimensional Metal-Containing Supramolecular Networks. *Coord. Chem. Rev.* **2016**, 308, 1–21.
- (9) Cooke, S. A.; Cotti, G.; Evans, C. M.; Holloway, J. H.; Legon, A. C. The Pre-reactive Complex H<sub>2</sub>O····ClF Identified in Mixtures of Water Vapour and Chlorine Monofluoride by Rotational Spectroscopy. *Chem. Commun.* **1996**, No. 20, 2327–2328.
- (10) Clark, T.; Hennemann, M.; Murray, J. S.; Politzer, P. Halogen Bonding: The Sigma-Hole. J. Mol. Model. 2007, 13 (2), 291–296.
- (11) Murray, J. S.; Politzer, P. The Electrostatic Potential: An Overview. Wiley Interdiscip. Rev. Comput. Mol. Sci. 2011, 1 (2), 153–163.
- (12) Zhang, X. X.; Liu, G. X.; Ciborowski, S.; Wang, W.; Gong, C.; Yao, Y. F.; Bowen, K. Spectroscopic Measurement of a Halogen Bond Energy. *Angew. Chem., Int. Ed.* **2019**, *58* (33), 11400–11403.
- (13) Cappelletti, D.; Candori, P.; Pirani, F.; Belpassi, L.; Tarantelli, F. Nature and Stability of Weak Halogen Bonds in the Gas Phase: Molecular Beam Scattering Experiments and Ab Initio Charge Displacement Calculations. *Cryst. Grow. Des.* **2011**, *11* (10), 4279–4283
- (14) De Santis, M.; Nunzi, F.; Cesario, D.; Belpassi, L.; Tarantelli, F.; Cappelletti, D.; Pirani, F. Cooperative Role of Halogen and Hydrogen Bonding in the Stabilization of Water Adducts with Apolar Molecules. *New J. Chem.* **2018**, 42 (13), 10603–10614.
- (15) Mason, K. A.; Pearcy, A. C.; Attah, I. K.; Platt, S. P.; Aziz, S. G.; El-Shall, M. S. Gas Phase Hydration of Halogenated Benzene Cations. Is it Hydrogen or Halogen Bonding? *Phys. Chem. Chem. Phys.* **2017**, 19 (28), 18603–18611.
- (16) Pearcy, A. C.; Mason, K. A.; El-Shall, M. S. Ionic Hydrogen and Halogen Bonding in the Gas Phase Association of Acetonitrile and Acetone with Halogenated Benzene Cations. *J. Phys. Chem. A* **2019**, 123 (7), 1363–1371.
- (17) Gillis, E. A. L.; Demireva, M.; Sarwar, M. G.; Chudzinski, M. G.; Taylor, M. S.; Williams, E. R.; Fridgen, T. D. Structure and Energetics of Gas Phase Halogen-Bonding in Mono-, Bi-, and Tridentate Anion Receptors as Studied by BIRD. *Phys. Chem. Chem. Phys.* **2013**, *15* (20), *7638*–*7647*.

- (18) Legon, A. C. Prereactive Complexes of Dihalogens XY with Lewis Bases B in the Gas Phase: A Systematic Case for the Halogen Analogue B XY of the Hydrogen Bond B HX. *Angew. Chem., Int. Ed.* 1999, 38 (18), 2686–2714.
- (19) Stephens, S. L.; Walker, N. R.; Legon, A. C. Rotational Spectra and Properties of Complexes B = ICF<sub>3</sub> (B = Kr or CO) and a Comparison of the Efficacy of ICl and ICF<sub>3</sub> as Iodine Donors in Halogen Bond Formation. *J. Chem. Phys.* **2011**, *135* (22), 224309.
- (20) Stephens, S. L.; Mizukami, W.; Tew, D. P.; Walker, N. R.; Legon, A. C. The Halogen Bond Between Ethene and a Simple Perfluoroiodoalkane: C<sub>2</sub>H<sub>4</sub>=ICF<sub>3</sub> Identified by Broadband Rotational Spectroscopy. *J. Mol. Spectrosc.* **2012**, 280, 47–53.
- (21) Springer, S. D.; Rivera-Rivera, L. A.; McElmurry, B. A.; Wang, Z. C.; Leonov, I. I.; Lucchese, R. R.; Legon, A. C.; Bevan, J. W. CMM-RS Potential for Characterization of the Properties of the Halogen-Bonded OC-Cl<sub>2</sub> Complex, and a Comparison with Hydrogen-Bonded OC-HCl. *J. Phys. Chem. A* **2012**, *116* (4), 1213–1223.
- (22) Evangelisti, L.; Feng, G.; Gou, Q.; Grabow, J. U.; Caminati, W. Halogen Bond and Free Internal Rotation: The Microwave Spectrum of CF<sub>3</sub>Cl-Dimethyl Ether. *J. Phys. Chem. A* **2014**, *118* (3), 579–582.
- (23) Flowers, B. A.; Francisco, J. S. Ab Initio Characterization of the Structure, Vibrational, and Energetic Properties of Br<sup>-</sup>·HOCl, Cl<sup>-</sup>·HOBr, and Br<sup>-</sup>·HOBr Anionic Complexes. *J. Phys. Chem. A* **2001**, *105* (2), 494–500.
- (24) Stropoli, S. J.; Khuu, T.; Boyer, M. A.; Karimova, N. V.; Gavin-Hanner, C. F.; Mitra, S.; Lachowicz, A. L.; Yang, N.; Gerber, R. B.; McCoy, A. B.; Johnson, M. A. Electronic and Mechanical Anharmonicities in the Vibrational Spectra of the H-bonded, Cryogenically Cooled  $X^-\text{HOCl}$  (X = Cl, Br, I) Complexes: Characterization of the Strong Anionic H-bond to an Acidic OH Group. *J. Chem. Phys.* Submitted for publication.
- (25) Roscioli, J. R.; Diken, E. G.; Johnson, M. A.; Horvath, S.; McCoy, A. B. Prying Apart a Water Molecule with Anionic H-Bonding: A Comparative Spectroscopic Study of the  $\bar{X} \cdot H_2O$  (X = OH, O, F, Cl, and Br) Binary Complexes in the 600–3800 cm<sup>-1</sup> Region. *J. Phys. Chem. A* **2006**, *110* (15), 4943–4952.
- (26) Peterson, K. A.; Figgen, D.; Goll, E.; Stoll, H.; Dolg, M. Systematically Convergent Basis Sets with Relativistic Pseudopotentials. II. Small-Core Pseudopotentials and Correlation Consistent Basis Sets for the Post-d Group 16–18 Elements. *J. Chem. Phys.* **2003**, 119 (21), 11113–11123.
- (27) Peterson, K. A.; Shepler, B. C.; Figgen, D.; Stoll, H. On the Spectroscopic and Thermochemical Properties of ClO, BrO, IO, and Their Anions. *J. Phys. Chem. A* **2006**, *110*, 13877–13883.
- (28) Boyer, M. A.; McCoy, A. B. A Flexible Approach to Vibrational Perturbation Theory Using Sparse Matrix Methods. *J. Chem. Phys.* **2022**, *156*, 054107.
- (29) Boyer, M. A.; McCoy, A. B. PyVibPTn, a General Package for Vibrational Perturbation Theory, 2021.
- (30) Yang, N.; Duong, C. H.; Kelleher, P. J.; Johnson, M. A.; McCoy, A. B. Isolation of Site-Specific Anharmonicities of Individual Water Molecules in the  $I^-(H_2O)_2$  Complex Using Tag-Free, Isotopomer Selective IR-IR Double Resonance. *Chem. Phys. Lett.* **2017**, *690*, 159–171.
- (31) Menges, F. S.; Perez, E. H.; Edington, S. C.; Duong, C. H.; Yang, N.; Johnson, M. A. Integration of High-Resolution Mass Spectrometry with Cryogenic Ion Vibrational Spectroscopy. *J. Am. Soc. Mass Spectrom.* **2019**, *30* (9), 1551–1557.
- (32) Wolk, A. B.; Leavitt, C. M.; Garand, E.; Johnson, M. A. Cryogenic Ion Chemistry and Spectroscopy. *Acc. Chem. Res.* **2014**, 47 (1), 202–210.
- (33) Kamrath, M. Z.; Garand, E.; Jordan, P. A.; Leavitt, C. M.; Wolk, A. B.; Van Stipdonk, M. J.; Miller, S. J.; Johnson, M. A. Vibrational Characterization of Simple Peptides Using Cryogenic Infrared Photodissociation of H<sub>2</sub>-Tagged, Mass-Selected Ions. *J. Am. Chem. Soc.* **2011**, *133* (16), 6440–6448.
- (34) Khuu, T.; Yang, N.; Johnson, M. A. Vibrational Spectroscopy of the Cryogenically Cooled O- and N-Protomers of 4-aminobenzoic

- Acid: Tag Effects, Isotopic Labels, and Identification of the E, Z Isomer of the O-Protomer. Int. J. Mass Spectrom. 2020, 457, 457.
- (35) Ashby, R. A. Infrared Spectrum of HOCl. J. Mol. Spectrosc. 1967, 23 (4), 439-447.
- (36) Barnes, I.; Becker, K. H.; Starcke, J. FTIR Spectroscopic Observation of Gaseous HOI. *Chem. Phys. Lett.* **1992**, 196 (6), 578–583
- (37) Berzinsh, U.; Gustafsson, M.; Hanstorp, D.; Klinkmuller, A.; Ljungblad, U.; Martenssonpendrill, A. M. Isotope Shift in the Electron-Affinity of Chlorine. *Phys. Rev. A* **1995**, *51* (1), 231–238.
- (38) Pelaez, R. J.; Blondel, C.; Delsart, C.; Drag, C. Pulsed Photodetachment Microscopy and the Electron Affinity of Iodine. *J. Phys. B* **2009**, 42 (12), 125001.
- (39) Markovich, G.; Pollack, S.; Giniger, R.; Cheshnovsky, O. Photoelectron Spectroscopy of Cl<sup>-</sup>, Br<sup>-</sup>, and I<sup>-</sup> Solvated in Water Clusters. *J. Chem. Phys.* **1994**, *101*, 9344–9353.
- (40) Serxner, D.; Dessent, C. E. H.; Johnson, M. A. Precursor of the  $I^{-aq}$  Charge-Transfer-to-Solvent (CTTS) Band in  $I^{-}(H_2O)_n$  Clusters. *J. Chem. Phys.* **1996**, 105, 7231–7234.
- (41) Wigner, E. P. On the Behavior of Cross Sections Near Thresholds. *Phys. Rev.* **1948**, 73, 1002–1009.
- (42) Yang, N.; Khuu, T.; Mitra, S.; Duong, C. H.; Johnson, M. A.; DiRisio, R. J.; McCoy, A. B.; Miliordos, E.; Xantheas, S. S. Isolating the Contributions of Specific Network Sites to the Diffuse Vibrational Spectrum of Interfacial Water with Isotopomer-Selective Spectroscopy of Cold Clusters. J. Phys. Chem. A 2020, 124 (50), 10393–10406.
- (43) Ashby, R. A. Infrared Spectrum of HOCl. J. Mol. Spectrosc. 1971, 40 (3), 639-640.
- (44) Towns, J.; Cockerill, T.; Dahan, M.; Foster, I.; Gaither, K.; Grimshaw, A.; Hazlewood, C.; Lathrop, S.; Lifka, D.; Peterson, G. D.; Roskies, R.; Scott, J. R.; Wilkins-Diehr, N. XSEDE: Accelerating Scientific Discovery. *Comput. Sci. Eng.* **2014**, *16* (5), 62–74.

